Interplay between salience and default mode network
in a socio-cognitive task towards a close other

Cátia Daniela Marques Ribeiro

UMinho | 2021

Universidade do Minho
Escola de Psicologia

Cátia Daniela Marques Ribeiro

Interplay between salience and default mode network in a socio-cognitive task towards a close other

junho de 2021

Universidade do Minho
Escola de Psicologia

Cátia Daniela Marques Ribeiro

Interplay between salience and default mode network in a socio-cognitive task towards a close other

Dissertação de Mestrado
Mestrado Integrado em Psicologia

Trabalho efetuado sob a orientação de
Professora Doutora Joana Fernandes Coutinho
Professor Doutor José Miguel Soares

junho de 2021

DIREITOS DE AUTOR E CONDIÇÕES DE UTILIZAÇÃO DO TRABALHO POR TERCEIROS

Acknowledgments

I want to dedicate this work to everyone that somehow have aided me during the last years:

To my supervisors, Professor Dr. Joana Fernandes Coutinho and Professor Dr. José Miguel Soares. Thank you, from the bottom of my heart, for the time, support, and unmeasurable help throughout this process. I learned so much from you, and without both your scientific and methodological expertise, this work could never be done.

To my dear sisters, Tânia and Vanessa, thank you for all the love, patience and support, in the roughest moments.

To my favorite uncle, Tio Carlos, thank you for always believing in me and for pushing me to grow into a better version of myself.

Finally, and for most, to the love of my life, Ricardo, thank you for all the love, understanding, and encouragement and for always being there.

I also would like to thank all the team from the Psychological Neuroscience Lab, especially Alberto Lema that kindly sent me some essential material. Unfortunately, I didn't have the chance to spend time at the lab, but I learned a lot from all the excellent presentations and discussions during our weekly neurolab meetings.

Additionally, a special thank you to my friends Isabela, Márcia, and Filipa, for all the support, good talks, and for the "ear" to my random lamentations.

STATEMENT OF INTEGRITY

I hereby declare having conducted this academic work with integrity. I confirm that I have not used plagiarism or any form of undue use of information or falsification of results along the process leading to its elaboration.

I further declare that I have fully acknowledged the Code of Ethical Conduct of the University of Minho.

University of Minho, 02.06.2021.

Interação entre *salience* e *default mode network* numa tarefa de cognição social com um outro significativo

Resumo

A cognição social - uma competência essencial no contexto das relações interpessoais - depende de dois subsistemas principais para a compreensão dos outros. Estes subsistemas são sustentados por diferentes redes cerebrais: a *Default Mode Network* (DMN), associada ao subsistema socio-cognitivo (i.e.,Mentalização), e a *Salience Network* (SN), associada ao subsistema socio-afetivo (i.e., Empatia). Estas correspondem a conhecidas redes cerebrais de descanso, que parecem constituir a base para a performance de tarefas sociais. Este estudo teve como objetivo analisar os mapas de conectividade funcional de ambas as redes na transição do estado de repouso para o desempenho de uma tarefa, utilizando para isso análise de componentes independentes e análise de conetividade baseada em *seeds.* 42 participantes envolvidos num relacionamento amoroso monogâmico responderam a um questionário de empatia diádica e foram submetidos a um protocolo fMRI, que incluiu uma aquisição de estado de repouso seguida por uma tarefa, na qual os sujeitos assistiam a vídeos com conteúdo emocional do seu parceiro, elaborando sobre a experiência do parceiro (condição *other*) ou sobre sua própria experiência (condição *self*). Verificámos que algumas regiões da DMN exibiram maior conectividade durante o desempenho da tarefa em comparação com o estado de repouso. A conectividade da SN foi mais limitada na condição *other* em comparação com as condições de repouso e *self.* Os resultados revelaram também uma interação entre a DMN e a SN, particularmente evidente durante o desempenho da tarefa social.

Palavras-chave: Cognição Social; *Default Mode Network*; *Other*; *Salience Network*; *Self.*

Interplay between salience and default mode network in a social-cognitive task towards a close other

Abstract

Social cognition, an essential ability in the context of interpersonal relationships, relies on two main subsystems to construct the understanding of others. These subsystems are sustained by different brain networks: the Default Mode Network (DMN) associated with the socio-cognitive subsystem (i.e., mentalizing), and the Salience Network (SN) associated with the socio-affective subsystem (i.e., empathy). These are well-known resting state networks that seem to constitute a baseline for the performance of social tasks. The present study aimed to investigate both networks' functional connectivity maps in the transition from rest to task performance, using independent component and seed-based analysis. A sample of 42 participants involved in a monogamous romantic relationship completed a questionnaire of dyadic empathy and underwent an fMRI protocol that included a resting state acquisition, followed by a task in which subjects watched emotional videos of their romantic partner and elaborated on their partner's (other condition) or on their own experience (self condition). We found that some DMN regions exhibited increased connectivity during task performance in comparison to resting state. The other condition revealed a more limited SN´s connectivity in comparison to the self and rest conditions. Overall, the results showed an interplay between the DMN and SN, particularly in social task performance.

Keywords: Social Cognition; Default Mode Network; Other; Salience Network; Self.

Contents

Abbreviations and acronyms

ACC - anterior middle cingulate cortex

AI - anterior insula

BOLD - blood oxygen level depend

DMN - Default Mode Network

EC - dyadic empathic concern subscale

FC - functional connectivity

fMRI - functional magnetic resonance imaging

ICA - independent component analysis

IFG - inferior frontal gyrus

IRIC - Interpersonal Reactivity Index for Couples

MCC - anterior middle cingulate cortex

MPFC - medial prefrontal cortex

PCC - posterior cingulate cortex

PT - dyadic perspective taking subscale

SC - Social cognition

SMFG - superior medial frontal gyrus

SN - Salience Network

TPJ - temporoparietal junction

List of figures

List of tables

Interplay between salience and default mode network in a social-cognitive task towards a close other

Introduction

Humans are highly social beings whose general welfare depends on the quality of the relationships established with others. Social cognition (SC) is, thus, the ability underlying the most significant human interactions, allowing us to understand our own and others' mental states, anticipate their actions, and act accordingly (Lieberman et al., 2019; Schurz et al., 2020; Van Overwalle, 2009). This ability is essential for adaptative interpersonal relationships, including those that we establish with significant or close others. Hence, SC is also crucial for the context of romantic relationships, whose healthy functioning critically depends on the partners' social-cognitive skills. For instance, partners who try to understand, share and respond to the other's feelings tend to be more satisfied with the relationship (Cohen et al., 2012; Péloquin & Lafontaine, 2010; Waldinger et al., 2004).

In social neuroscience, SC is conceptualized as a multidimensional construct that relies on two main subsystems, or routes, to construct the understanding of others (Kanske et al., 2015; 2016). The affective subsystem, commonly referred to in the literature as empathy or affective empathy, is responsible for our ability to experience or share the other person's emotional states (de Vignemont & Singer, 2006; Kanske et al., 2015; Walter, 2012). The cognitive subsystem, generally addressed as mentalizing, theory of mind, or cognitive empathy, is responsible for our capacity to cognitively represent and understand others' mental and affective states (Frith & Frith, 2005; Schurz et al., 2014; Walter, 2012). Thus, SC involves both low-level embodied and high-level inference-based processes.

Over the last decades, researchers have relayed on imaging techniques, such as functional magnetic resonance imaging (fMRI), to investigate the neural basis of these two routes of social processing. Several experimental studies using different social tasks, as well as recent metanalysis (Schurz et al., 2020), have shown that empathy and mentalizing are subserved by different functional brain networks, which have been replicated in resting state activity, as well (Kanske et al., 2015; Alcalá-López et al., 2018).

The affective subsystem of SC has been mainly associated with regions such as the anterior insula (AI), inferior frontal gyrus, anterior (ACC) and middle cingulate cortex (MCC), supplementary motor area, amygdala, and thalamus (Bzdok et al., 2012; Fan et al., 2011; Kanske et al., 2015). These regions largely overlap with the Salience Network (SN), a resting state network anchored in the AI and dorsal ACC (dACC) that also comprises the amygdala, ventral striatum, and the substantia nigra/ventral tegmental area (Menon, 2015; Seeley et al., 2007).

The SN is responsible for salience attribution and integration of internal (autonomic, visceral, and somatic) and external cues to guide the emotional, interpersonal, and self-processing (Menon, 2015; Menon & Uddin, 2010; Sevinc et al., 2017). The AI and dACC are typically associated with socio-affective tasks involving general forms of empathy, empathy for pain, and other interoceptive processes (Fallon et al., 2020; Timmers et al., 2018). For example, a study by Cheng and colleagues (2010) demonstrated that both regions were highly activated when the participants had to imagine a loved-one in pain, compared to imagining a stranger in the same situation, which was recently replicated by López-Solà and her team (2020).

As pointed by Nomi et al. (2016), the AI is a specific hub for affective processing and cognitive control, with connections to frontal, anterior cingulate, and parietal regions. Furthermore, coactivations of both the AI and ACC are observed during the emotional processing of a wide range of states from disgust to fear or anger (Craig, 2010), which highlights the role of the SN in the affective subsystem.

On the other hand, the cognitive subsystem is subserved by a series of brain regions associated with the mental representations of ourselves and others, namely the medial prefrontal cortex (MPFC), posterior cingulate cortex (PCC) and adjacent precuneus, temporoparietal junction (TPJ), temporal pole, superior temporal sulcus and inferior parietal lobule (Bzdok et al., 2012; Kanske et al., 2015; Schilbach et al., 2012). These regions present a clear anatomical overlap with the brain's Default Mode Network (DMN), one of the most studied resting state networks, that usually exhibits higher activity at rest than during task performance (Di & Biswal, 2014; Greicius et al., 2003; Raichle, 2015). Notably, some psychological tasks yield little or no deactivation of the DMN compared to resting periods (Buckner, 2012). In fact, the DMN has been shown to keep consistently activated in a wide range of socio-cognitive processes such as mentalizing and mental state attribution, as well as emotion processing, moral cognition, episodic and autobiographic memory, amongst others (Amft et al., 2015; Chiong et al., 2013; Li et al., 2014; Spreng & Andrews-Hanna, 2015).

Indeed, the connection between the DMN and SC was consistently reported in various studies (Mars et al., 2012), including the ones showing its positive association with pro-social personality traits like extraversion and agreeableness (Coutinho et al., 2013, Sampaio et al., 2014,) and self-perceived empathy (Oliveira-Silva et al. 2018; Esménio et al., 2019b). Taken together, these evidences support the critical role of this network in our ability to infer emotional and cognitive states.

The close relationship between these resting state networks and SC, especially with the DMN, have led some authors to suggest that the brain´s dynamics at rest may work as a physiological baseline that prepares us to adaptively respond to things social in nature, the most behaviorally relevant stimuli for humans (Meyer, 2019; Northoff et al., 2010; Schilbach et al., 2008). This is in line with data showing that the resting state activity facilitates subsequent social task performance activity (Meyer & Lieberman, 2018; Spunt et al., 2015).

In sum, evidence from both task performance and resting state highlights the role of the two SC related networks to construct the understanding of ourselves and others. However, what is less known is how the functional organization of these social brain networks change in the transition from rest to the performance of a social task, either in terms of the reconfiguration of each network´s architecture and in terms of the dynamic interactions between both networks.

The present study was designed to address this question by looking at the changes from resting state to task performance, within each network, as well as the changes in the interplay between the DMN, as a top-down mentalizing brain network, and the SN, as a bottom-up affective processing network in SC. Importantly, the social task (described in the method section) includes a self and close other condition. The emotional proximity with the target should influence the configuration of the networks under study across the experimental conditions due to the known anatomical overlap between self and close other processing (Esménio et al. 2019a). For example, the MPFC, a DMN region known to be particularly active when thinking about the self (Huang et al., 2016), is also active when thinking about a close other, particularly its ventral portion (Krienen et al., 2010)). Likewise, Courtney and Meyer (2020), in their work about the way the brain organizes representations of others based on their proximity to the self, reported a self-other overlap in the main DMN's nodes, such as MPFC and PCC/precuneus.

Indeed, most social situations require both emotional sharing and mental state understanding abilities. Hence, these two networks are likely to work together, as demonstrated in previous studies focused on the cross-network interactions in socio-cognitive tasks (Schurz et al., 2021). For example, a study by Meyer and colleagues (2013) found significant functional connectivity (FC) between the MPFC and dACC and insula in situations where participants observed a friend experiencing social exclusion compared to a stranger. In the same line, Kanske and collaborators (2016) demonstrated that the two networks appeared to interact during the performance of a social task. Specifically, they found that during highly emotional situations, the AI inhibited the TPJ activity, which according to the authors may indicate that in situations where empathizing and mentalizing are required, the former ability may be prioritized over the latter.

In this study, we used two complementary approaches to analyze the pattern of FC: independent component analysis (ICA), a purely data-driven method that provides information about whole-brain functional networks (Soares et al., 2016), and seed-based correlation analyses, a method to identify correlations in brain activity of specific seed regions with other brain areas (Von dem Hagen et al. 2013).

Regarding the FC of the DMN, we hypothesize that the spatial maps of the network, extracted using ICA, will present the traditional nodes composing the DMN in the three conditions (rest, self, and other). Due to the nature of the social task, which requires clear mentalization, the FC of the DMN may even increase in the transition from rest to task, with the traditional mentalizing regions such the MPFC, PCC/precuneus and TPJ, exhibiting greater FC in the self and other conditions in comparison to rest.

Likewise, we also hypothesize that the SN will exhibit the typical FC map during rest, self, and other processing. Moreover, due to the role of this network, namely the AI and ACC nodes, for self-interoceptive processes and the integration of physiological changes and bodily sensations, we expect to find a greater FC in these regions in the self condition.

Regarding the interplay between networks, we hypothesize that when seeding the MPFC as a core region of the DMN and the right AI as a core region of the SN, we will observe increased connectivity between this seed and the areas of the SN, during the self condition, in comparison to the other condition. Additionally, we anticipate an increased FC between the AI and posterior regions of the DMN in the other condition.

Finally, in terms of how the FC of these two social brain networks is associated with self-reported scores on the affective and cognitive dimensions of SC, we anticipate that the connectivity within the DMN will be positively correlated with the scores in the cognitive dimension and that the connectivity within the SN will be associated with the scores in the affective dimension.

Method

Participants

Forty-two (20 females) caucasian subjects in a committed monogamous romantic relationship for at least one year participated in this study. The participants were recruited through a snowball sampling method. Before any procedure, inclusion and exclusion criteria were assessed during a preliminary screening interview conducted over the telephone. The inclusion criteria were: age between 20 and 50 years old; right-handed; no prior or concurrent diagnosis of any neurological or psychiatric disorder; not dependent on alcohol and/or drugs in the last year; ability to attend a magnetic resonance imaging (MRI) screening session (e.g., absence of metallic implants, pregnancy, etc.). The majority of the participants had college degrees (78.95%) and their ages ranged from 23 to 39 years old (*M* = 31.08, *SD* = 4.73; for males: *M* = 31.57, *SD* = 8.32; and for females *M* = 30.47, *SD* = 8.58).

Self-report measures

Before the experiment, participants completed a set of self-report measures of empathy and dyadic adjustment. In this study, we focused on the Portuguese version of the *Interpersonal Reactivity Index for Couples* (IRIC) to assess socio-cognitive skills in the context of the relationship. This instrument, originally developed by Péloquin and LaFountaine (2010), and adapted to Portuguese by Coutinho et al. (2015a), is a modified version of the *Interpersonal Reactivity Index* (Davis, 1980) that assesses cognitive and emotional empathy in the context of intimate relationships. It contains thirteen items evaluated on a five-point Likert scale, divided into two subscales. The *dyadic perspective taking subscale* (PT) is composed by six items that measure the tendency to spontaneously adopt the partner's points of view. The *dyadic empathic concern subscale* (EC) is composed by seven items and focuses on the feelings of sympathy and concerns oriented towards the partner in unfortunate situations.

The IRIC (α = 0.82) total score varies between 0 and 52, with higher scores indicating higher perceived dyadic empathy abilities. The score of PT (α = 0.85) ranges between 0 and 24, and the score of EC (α = 0.67) ranges between 0 and 28. Detailed participants' scores can be found in Table 1.

Table 1

Participants' IRIC total scores and respective subscales scores

Scale and subscales	**Range**	***M***	***SD***
IRIC Total	32 - 49	40.26	4.58
IRIC-PT	7 - 24	16.21	3.54
IRIC-EC	19 - 27	24.05	2.55

Note. IRIC = Interpersonal Reactivity Index for Couples; PT = dyadic perspective taking subscale; EC = dyadic empathic concern subscale; *M* = mean; *SD* = standard deviation.

Experimental procedure

After the first screening to assess the inclusion in the study, the goals and procedures were explained to the participants, who signed a written informed consent before the beginning of the experiment. This study belongs to a large research project about social cognition in the context of romantic interaction, which was approved by the Institutional Review Board of University of Minho and complied with the principles expressed in the Declaration of Helsinki (with the amendment of Tokyo 1975, Venice1983, HongKong 1989, Somerset West 1996, Edinburgh 2000).

The experiment started with each participant completing a sociodemographic form and the self-report measures. Then, after assured all the security measures, each participant went on a fMRI scanning session at a clinical hospital in Oporto. While being scanned, the participants performed the social task described below. The total experimental procedure time lasted 45 minutes.

Image acquisition

Structural (T1) and functional (T2*) images were acquired with a clinically approved 3 Tesla MRI scanner (Siemens Magnetom Skyra, Erlangen, Germany) in one imaging session per participant. Each session included one MPRAGE T1 scan (192 sagittal slices) with the following parameters: repetition time (TR) = 2000 ms; echo time (TE) = 2.33s; flip angle (FA) = 7°; field of view (FoV) = 256 mm; slice gap = 0 mm; pixel size = 0.8×0.8 mm^2; and slice thickness = 0.8 mm and one functional blood oxygen level depend (BOLD) sensitive echo-planar imaging (EPI) sequence (375 volumes; 39 axial slices) with the subsequent imaging parameters: TR = 2000 ms; TE = 29 ms; FA = 90°; FoV = 1554 mm; matrix size = 64×64; pixel size = 3×3 mm^2; and slice thickness = 3 mm. During this sequence, the synchronization between the experimental paradigm and the acquisition for each TR was ensured using the Lumina 3G Controller. Additionally, before the experimental task a 7 minutes resting state functional (T2*) scan (210 volumes; 39 axial slices) was acquired following the same EPI parameters. During the resting state/task-free acquisition, participants were instructed to keep their eyes closed, to remain awake but relaxed and motionless as possible, doing nothing in particular during the acquisition.

Socio-cognitive task

Each participant watched a set of video vignettes (20 seconds) of his/her romantic partner expressing emotional content. While watching the vignettes, participants were asked to either focus on their own experience (self condition) or on their partner's experience (other condition). These videos containing negative and positive emotional content towards the partner were extracted from a previously video-recorded interaction task in the lab (details regarding this interaction task can be found in Coutinho et al., 2017; 2018).

The task was composed by two blocks, one for each condition, and each block contained 22 trials. Each trial was composed by a fixation cross (during 5 seconds); instructions in accordance with each referent block, for example the instruction for the other block was "In the next video focus on how your partner is feeling."; during (3 seconds); video (during 20 seconds); and behavioral response (during 4 seconds). An example of a trial in the other condition is displayed in Figure 1.

In terms of the behavioral response (which essentially aimed to ensure that participants were focusing in their own and on the partner's experience) it was required to participants to choose among one of three options, dependent on the emotional impact of the video: "Bad" for any kind of negative state or emotion, "Neutral" in the absence of any positive or negative state or emotion; or "Good" for any kind of positive state or emotion.

The stimuli were displayed in a pseudo-randomized order. The blocks were also displayed in a randomized order across participants. The total duration of the task was 1364 seconds (24 minutes). More detailed information regarding this task can be found in Esménio et al. (2019; 2020).

Figure 1

Example of a trial on the other condition

Data analysis

Image processing

Before data processing, all images were visually inspected to ensure the absence of head motion artifacts and any brain lesion. All imaging were preprocessed using the advanced edition of the Data Processing Assistant for Resting-State fMRI 5.1 (DPARSF; Chao-Gan & Yu-Feng 2010; http://rfmri.org/DPARSF), according to the following steps: removal of the first five volumes (10s), to ensure signal stabilization and participants adjustment to scanner noise; slice-timing correction, using the middle slice as reference; motion correction, using rigid body alignment of each volume to the mean image of the acquisition and motion scrubbing (volumes in which FD > .5 and DVARS > .5% change in the BOLD signal were "scrubbed," or removed entirely from the data), to correct for movement artifacts and related susceptibility artifacts; rigid-body registration of the mean functional image to the T1 and segment using Diffeomorphic Anatomical Registration Through Exponentiated Lie Algebra (DARTEL; Ashburner, 2007); normalization to the Montreal Neurological Institute (MNI) space by DARTEL; smoothing with a Gaussian kernel of 8 mm full-width at half-maximum to decrease spatial noise; and band-pass temporal filtering (0.01-0.08 Hz), applied to the resting state functional images, and high-pass temporal filtering (128s) applied to the images acquired during task performance, to remove low-frequency noise from the data.

The final images were visually inspected and eight participants were excluded: one due to head motion higher than 2 mm in translation and 2° in rotation; two due to anatomical abnormalities; four due to technical problems during the acquisition; and one due to abnormal activation patterns/noise during task performance.

Independent Component Analysis

Group spatial independent component analysis (ICA) was carried out to search for common spatial patterns among subjects, both during resting state and during task performance, using the Group ICA v4.0c of fMRI Toolbox (GIFT; http://mialab.mrn.org/software/gift/).

The ICA analysis consisted in extracting the individual spatial independent maps and their related time courses (Beckmann et al., 2005). The dimensionality reduction of the functional data and computational load was performed with principal component analysis (PCA). The estimated number of independent components (IC) was 20, for each subject, based on a good trade-off between preserving the information in the data while reducing its size (Calhoun et al., 2001; Beckmann et al., 2005). ICA calculation was then performed using the iterative Infomax algorithm (Bell & Sejnowski, 1995). The ICASSO tool was used to control the ICA reliability. Twenty computational runs were made on the dataset, during which the components were being recomputed and compared across runs and the robustness of the results was ensured (Himberg et al., 2004).

The IC were obtained and each voxel of the spatial map was expressed as a *t* statistic map, which was finally converted to a *z* statistic that characterizes the degree of correlation of the voxel signal with the component time course, providing a measure of the FC within each network. Then, the IC were sorted, visually inspected and spatially matched using the DMN and SN templates, provided by FIND Lab (http://findlab.stanford.edu/functional_ROIs.html). We selected the IC that showed the highest spatial overlap with the provided templates, to represent each network.

For the group analysis (second-level analyses), the General Linear Model (GLM) from Statistical Parametric Mapping 12.0 (SPM12; Wellcome Department of Cognitive Neurology, London, UK; http://www.fil.ion.ucl.ac.uk) was used. The individual DMN and SN's *z* maps, were included in the same group and a one-sample *t* test ($p < .05$ FWE corrected and extent threshold k = 10 voxels) was performed to study the global pattern of activation of the DMN and SN. The resulting statistical maps were masked using the DMN and SN templates, respectively. Only the typical DMN and SN regions were reported and anatomical labeling was assigned by a combination of visual inspection and Anatomical Automatic Labeling atlas (AAL; Tzourio-Mazoyer et al., 2002).

Seed-based analysis

For the seed-based functional connectivity analysis, we used *a priori* defined ROIs, based on MNI coordinates reported by previous fMRI studies. Thus, for the DMN we selected the ventral MPFC (x = 1, y = 55, z = -3) following the coordinates proposed by Di & Biswal (2014) and Knyazev et al. (2020). As seed for the SN, we used the right AI (x = 36, y = 18, z = 4) following the coordinates proposed by Menon (2015) and Alcalá-López et al. (2018) using a 8 mm radius sphere in both cases.

The correlation maps for these seed regions were produced by computing correlation coefficients between the mean time series of each ROI and the time series of all other voxels in the brain for each participant. Correlation coefficients were converted to *z*-values using Fisher's transform to improve normality. Then, the individual participant's *z* maps from each seed were used to perform second-level analyses, following the same procedure described above, in the ICA section.

To study the interplay between the DMN and SN, we used the same individual z maps from each seed, including it in the same group and performed a one-sample *t* test ($p < .05$ FWE corrected and extent threshold k = 10 voxels), masking the resulting statistical map of the MPFC's seed with the template of the SN, and masking resulting statistical map of the rAI's seed with the template of the DMN.

Only the typical DMN and SN regions were reported and anatomical labeling was assigned by a combination of visual inspection and AAL.

Correlation analysis with IRIC

The multiple regression (with positive and negative correlations) was performed to identify which areas of the DMN and SN were associated with IRIC total, cognitive and affective scores. Results were considered significant at $p < .05$ corrected for multiple comparisons using the Monte Carlo correction (combined height threshold $p = .05$ and a minimum cluster size = 54 for the DMN and 35 for the SN determined by Monte Carlo simulation program, AlphaSim). The resulting statistical maps were, also, presented using the DMN and SN's templates as masks, and only the typical network regions were reported and anatomical labeling was assigned by a combination of visual inspection and AAL.

Results

DMN and SN's functional connectivity in Res, Self and Other conditions

Independent component analysis approach

DMN's functional connectivity

At a group level the DMN's spatial maps activated the traditional regions associated with this network, in the three conditions, as can be observed in table 2.

We found that the DMN's connectivity pattern changed from resting state to self and other processing, with some regions exhibiting increased FC during the social task performance, in comparison to resting state as can also be observed in table 2 and figure 2.

Moreover, we observed a higher FC in anterior regions of the DMN, namely in left superior medial frontal gyrus (SMFG) and ventral ACC both in rest and self conditions, and higher FC on posterior regions in the other condition, namely in PCC/precuneus.

SN's functional connectivity

Regarding the SN's connectivity, we found that the spatial maps also evidenced the traditional regions associated with this network, in the three conditions, as can be seen in table 3.

The overall network's FC pattern changed between conditions, with the other condition revealing a more limited SN´s connectivity in comparison to the self and rest conditions. For instance, the other condition presented a lower FC in the dorsal ACC - a SN's key region - and showed a reduced connectivity in the AI, as illustrated in figure 2.

Table 2

DMN's functional connectivity in the three conditions

		MNI Coordinates						**MNI Coordinates**						**MNI Coordinates**				
	Region of interest	**x**	**y**	**z**	**T**	**k**	**Region of interest**	**x**	**y**	**z**	**T**	**k**	**Region of interest**	**x**	**y**	**z**	**T**	**k**
DMN	*Resting*						*Self*						*Other*					
	L Superior medial frontal	-6	51	15	29.11	1038	L Ventral anterior cingulate	-3	45	15	45.09	1218	R Precuneus	6	-57	18	40.31	469
	R Ventral anterior cingulate	6	48	18	28.51		R Ventral anterior cingulate	9	45	18	44.54		L Posterior cingulate	0	-42	30	38.44	
	R Posterior cingulate	3	-48	27	19.05	347	L Precuneus	-3	-57	18	38.34	469	L Precuneus	-6	-54	18	37.47	
	L Posterior cingulate	-6	-51	27	18.27		R Precuneus	6	-57	18	37.30		R Ventral anterior cingulate	6	39	12	39.47	1189
	L Angular /TPJ	-48	-66	33	15.64	22	R Posterior cingulate	6	-42	21	31.64		L Ventral anterior cingulate	-3	42	9	38.89	
	R Superior frontal	15	36	51	14.97	40	L Angular/TPJ	-42	-66	33	29.07	22	L Angular/TPJ	-42	-66	33	30.21	22
	R Angular/TPJ	51	-63	27	13.55	13	R Angular/TPJ	51	-63	27	23.30	13	R Angular/TPJ	48	-60	30	27.04	13
							R Middle cingulate	3	-15	39	17.42	33	L Middle cingulate	0	-21	39	17.46	33
							L Parahippocampal	-24	-30	-12	16.49	79	R Superior frontal	18	42	39	13.75	31
							R Superior frontal	15	33	51	15.45	39	L Superior medial frontal	-3	51	15	13.46	446
							L Middle cingulate	0	-21	39	14.84	29	L Frontal medial orbital	0	51	-3	13.07	
							L Superior medial frontal	-3	60	12	14.02	547	R Middle cingulate	3	-15	39	13.17	32
							L Middle frontal	-24	30	48	10.69	43	L Lingual	-15	-33	-3	12.69	74
							L Thalamus	-6	-3	6	10.09	66	L Parahippocampal	-21	-24	-12	11.50	
							R Thalamus	6	-6	3	9.94		L Middle frontal	-24	30	48	11.28	79
													L Thalamus	-6	0	0	7.70	40
													R Thalamus	6	-15	3	7.49	

Note. p<.05 FWE corrected, extent threshold k=10 voxels; k = cluster size; L = left, R = right; TPJ = temporoparietal junction.

Table 3

SN's functional connectivity in the three conditions

		MNI Coordinates						**MNI Coordinates**						**MNI Coordinates**				
	Region of interest	**x**	**y**	**z**	**T**	**k**	**Region of interest**	**x**	**y**	**z**	**T**	**k**	**Region of interest**	**x**	**y**	**z**	**T**	**k**
SN	*Resting*						*Self*						*Other*					
	L Supplementary motor area	-6	15	54	23.61	819	L Middle frontal	-30	39	24	21.84	168	R Supplementary motor area	9	9	54	27.46	715
	R Anterior middle/ dorsal anterior cingulate	3	18	39	20.13		L Anterior middle/ dorsal anterior cingulate	-9	18	33	21.60	447	L Supplementary motor area	-6	9	57	25.07	
	L Anterior insula	-39	18	-9	18.38	98	R Anterior middle/dorsal anterior cingulate	9	21	36	19.25		L Middle frontal	-33	39	27	14.80	125
	R Anterior insula	45	18	-6	15.65	95	R Superior frontal	27	45	24	17.71	133	R Middle frontal	30	45	21	13.51	106
	L Superior frontal	-27	51	24	12.60	148	L Anterior Insula	-33	15	-3	14.63	94	L Anterior Insula	-30	24	3	10.45	16
	R Superior frontal	27	45	24	11.55	106	R Supplementary motor area	15	9	63	13.11	78						
							L Supplementary motor area	-15	6	63	12.82	42						
							R Anterior Insula	42	12	-3	12.46	96						

Note. p<.05 FWE corrected, extent threshold k=10 voxels; k = cluster size; L = left, R = right.

Figure 2

Group-level spatial patterns of the DMN and SN in the three conditions

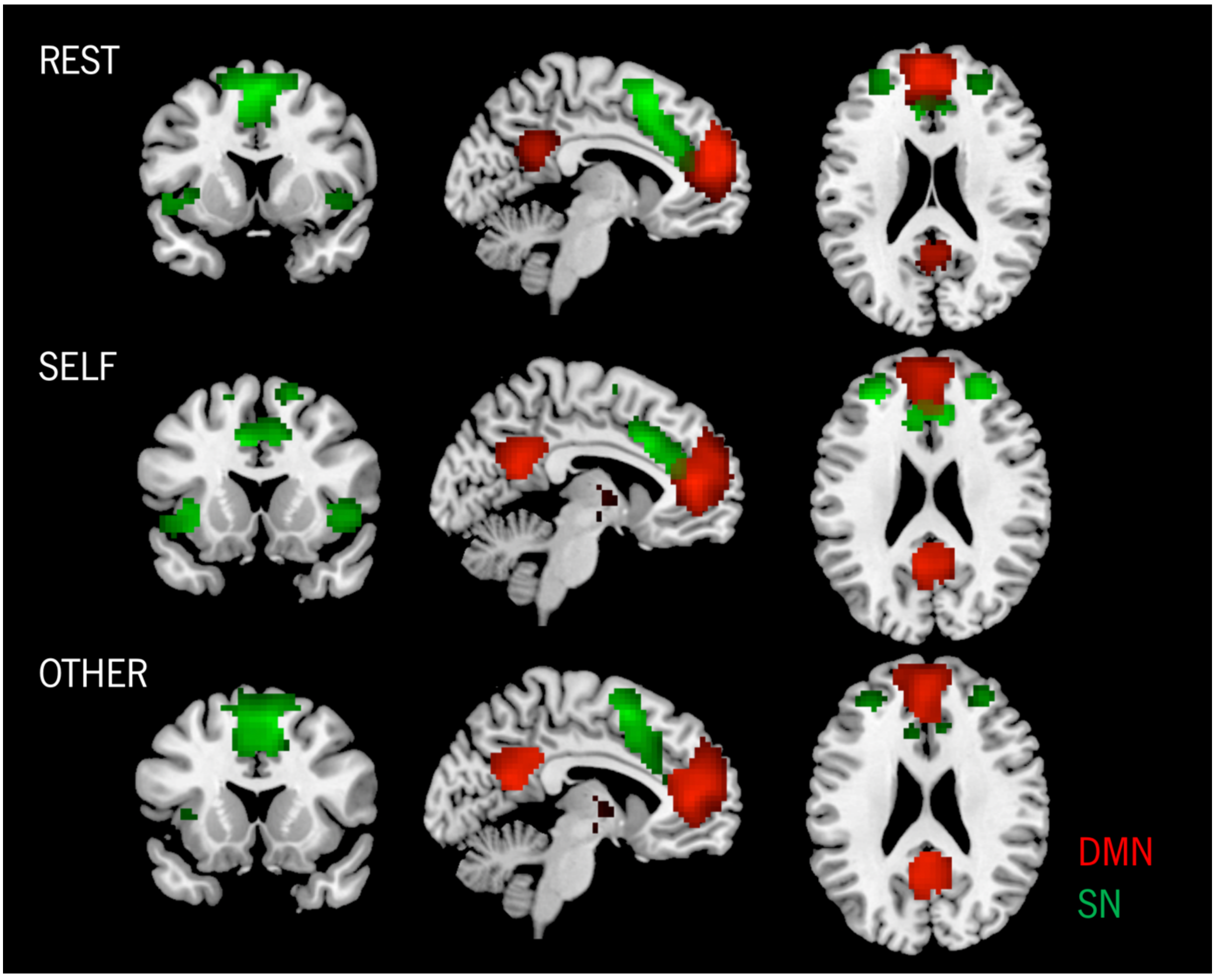

Note. p <.05 FWE corrected, extent threshold k=10 voxels.

Seed-based approach

MPFC's functional connectivity with overall DMN

We found that the MPFC, the selected DMN´s seed region, showed significant FC with the other traditional regions of the DMN, in the three conditions, as shown in table 4, however it appeared to be relatively stronger in the rest condition in comparison with the self and other conditions.

rAI's functional connectivity with overall SN

We found that the rAI, the selected SN's seed region, was also functionally connected with the other traditional regions of the SN, in the three conditions, as can be observed in table 5. Additionally, this seed region also exhibited increased FC with the left cerebellum in the three conditions.

Table 4

MPFC's functional connectivity with overall DMN

		MNI Coordinates						**MNI Coordinates**						**MNI Coordinates**				
Seed	**Connected region**	**x**	**y**	**z**	**T**	**k**	**Connected region**	**x**	**y**	**z**	**T**	**k**	**Connected region**	**x**	**y**	**z**	**T**	**k**
MPFC	*Resting*						*Self*						*Other*					
	L Frontal medial orbital	0	54	-3	561.28	1559	L Frontal medial orbital	0	54	-3	385.68	1563	L Frontal medial orbital	-3	54	-3	330	1528
	L Superior frontal	-18	39	48	17.13		R Ventral anterior cingulate	6	27	18	17.09		R Ventral anterior cingulate	6	27	18	14.4	
	L Posterior cingulate	-6	-48	30	25.00	469	L Middle frontal	-24	30	48	14.57		L Middle frontal	-24	27	51	12.8	
	L Precuneus	-3	-60	15	24.53		L Angular/TPJ	-39	-66	33	15.46	25	R Precuneus	6	-63	21	17.4	469
	L Angular/TPJ	-45	-66	33	22.96	25	R Precuneus	9	-51	36	15.29	469	R Posterior cingulate	6	-48	30	17.1	
	R Angular/TPJ	51	-60	30	20.21	13	R Posterior cingulate	3	-42	21	14.69		L Angular/TPJ	-39	-69	33	15.5	25
	L Middle cingulate	0	-21	36	17.97	34	L Cuneus	-9	-63	24	14.69		R Angular/TPJ	48	-63	33	14.5	13
	L Hippocampus	-24	-24	-12	16.23	115	R Superior frontal	15	33	51	13.94	40	R Middle cingulate	3	-21	39	12.4	34
	L Thalamus	-15	-33	3	15.70		R Middle cingulate	3	-21	39	13.32	34	L Middle cingulate	0	-9	36	11.4	
	R Superior frontal	18	42	45	14.50	40	R Angular/TPJ	48	-63	30	12.78	13	R Thalamus	6	-6	9	11.9	65
	R Parahippocampal	30	-27	-12	13.79	42	L Thalamus	-6	0	0	12.50	67	L Thalamus	-3	-9	9	11.3	
	R Thalamus	6	-6	9	9.62	67	R Thalamus	6	-6	9	10.38		R Superior frontal	15	33	51	11.5	40
							L Parahippocampal	-24	-24	-18	10.55	115	R Parahippocampal	27	-18	-18	10.1	42
							R Parahippocampal	27	-21	-18	9.01	41	L Parahippocampal	-21	-24	-12	8.90	116

Note. p<.05 FWE corrected, extent threshold k=10 voxels; k=cluster size; L = left, R = right; TPJ = temporoparietal junction.

Table 5

Right AI's functional connectivity with overall SN

		MNI Coordinates						MNI Coordinates						MNI Coordinates				
Seed	**Connected region**	**x**	**y**	**z**	**T**	**k**	**Connected region**	**x**	**y**	**z**	**T**	**k**	**Connected region**	**x**	**y**	**z**	**T**	**k**
R AI	*Resting*						*Self*						*Other*					
	R Anterior insula	36	21	3	577.8	101	R Anterior insula	36	18	3	549.27	101	R Anterior insula	36	18	3	589	101
	R Anterior middle/ dorsal anterior cingulate	6	18	36	69.26	865	L Anterior insula	-33	18	6	69.64	98	L Anterior insula	-36	12	6	73.4	98
	L Anterior middle/ dorsal anterior cingulate	-6	12	39	53.45		R Middle frontal	33	39	27	46.13	142	L Middle frontal	-39	45	15	33.6	181
	R Supplementary motor area	3	0	60	44.38		R Anterior middle/ dorsal anterior cingulate	6	12	45	36.26	864	R Middle frontal	36	39	27	32.5	142
	L Anterior insula	-30	21	3	48.76	98	L Supplementary motor area	-3	3	51	34.00		L Supplementary motor area	-3	3	51	30	855
	R Middle frontal	33	42	24	40.39	142	L Middle frontal	-33	39	33	32.76	181	R Supplementary motor area	3	0	57	29.3	
	L Middle frontal	-36	42	24	33.37	181	L Cerebellum	-30	-54	-30	11.89	27	L Cerebellum	-33	-54	-30	11.50	27
	L Cerebellum	-36	-54	-30	12.71	27												

Note. p<.05 FWE corrected, extent threshold k=10 voxels; k=cluster size; L = left, R = right.

Interplay between SN and DMN

When analyzing the FC between the MPFC and regions within the SN, we found that this seed was functionally connected with the traditional regions of the SN in the three conditions, as can be observed in the table 6. Moreover, we found that the FC between the MPFC and the AI, was reduced in the rest condition (see figure 3), in comparison to the self and other conditions. In the same way, the FC between MPFC and the dACC, another SN's key region, appeared to be increased in self and other conditions. Furthermore, we observed FC between this seed region and the cerebellum only in the task-dependent conditions.

Figure 3

Functional connectivity between MPFC and SN's regions in the three conditions

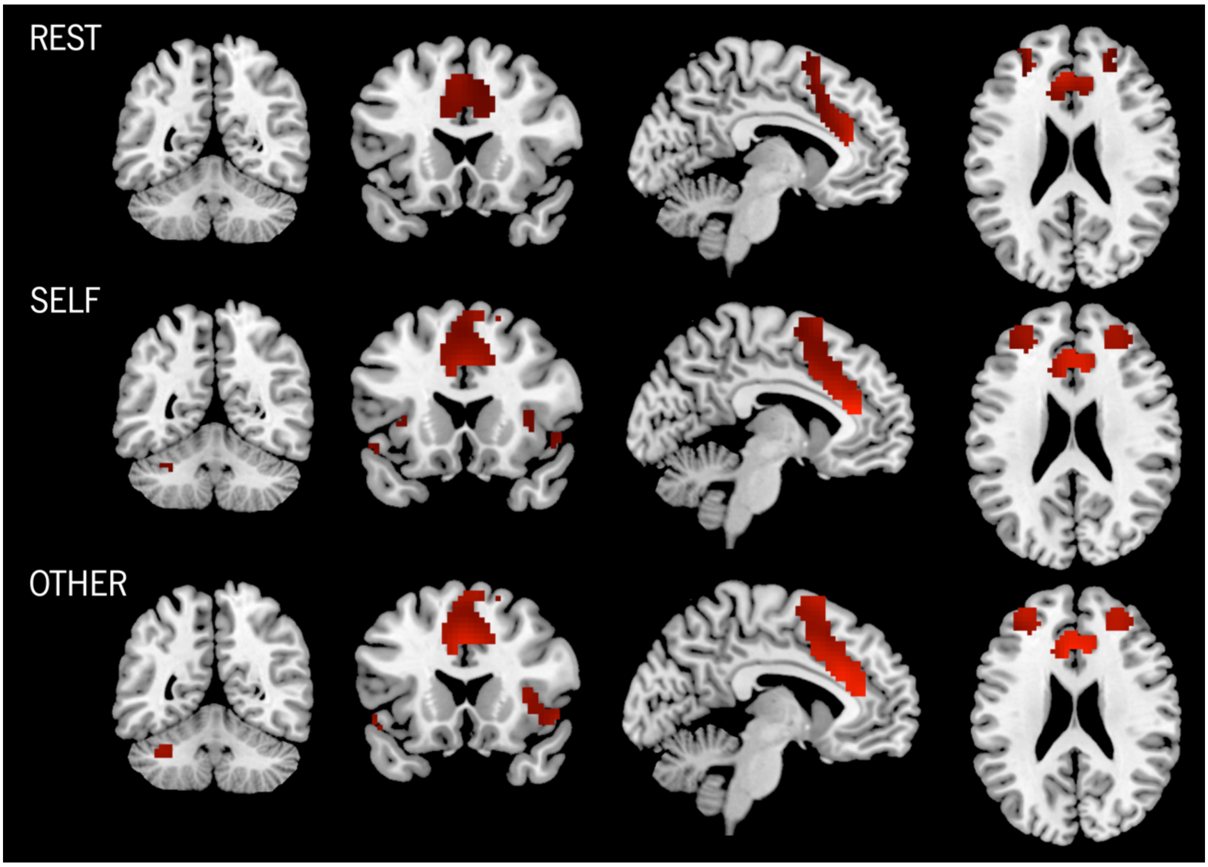

Note. p <.05 FWE corrected, extent threshold k=10 voxels.

Table 6

Functional connectivity between MPFC and SN's regions in the three conditions

		MNI Coordinates						MNI Coordinates						MNI Coordinates				
Seed	**Connected region**	**x**	**y**	**z**	**T**	**k**	**Connected region**	**x**	**y**	**z**	**T**	**k**	**Connected region**	**x**	**y**	**z**	**T**	**k**
MPFC	*Resting*						*Self*						*Other*					
	L Anterior Cingulate	-3	39	15	19.79	647	L Anterior Cingulate	-6	36	15	18.36	803	L Middle frontal	-27	51	9	15.5	181
	R Anterior Cingulate	9	36	18	14.53		R Anterior Cingulate	6	36	18	17.01		L Anterior Cingulate	0	27	27	15	806
	L Supplementary motor area	-6	15	66	12.88		L Middle frontal	-30	45	36	14.71	181	R Anterior Cingulate	6	27	21	14.3	
	L Middle frontal	-27	54	9	14.15	133	R Superior frontal	24	48	15	12.45	142	R Superior frontal	24	48	15	11.7	142
	R Middle frontal	24	39	30	10.01	77	R Middle frontal	30	48	33	11.77		R Middle frontal	27	42	33	11.1	
	R Superior frontal	24	48	15	8.8		R Anterior insula	33	21	3	7.75	89	L Cerebellum	-33	-60	-33	8.63	27
	L Frontal inferior orbital	-45	18	-12	9.53	32	R Frontal inferior operculum	51	12	6	6.71		R Frontal inferior orbital	51	18	-6	8.34	101
	R Anterior insula	36	15	-9	9.42	13	L Anterior insula	-30	21	3	7.18	59	R Anterior insula	33	21	3	7.81	
							L Superior temporal Pole	-48	18	-12	7.02		L Anterior insula	-30	24	3	6.9	25
							L Cerebellum	-30	-54	-30	6.86	24	L Superior temporal Pole	-48	18	-12	6.67	19

Note. $p<.05$ FWE corrected, extent threshold k = 10 voxels; k=cluster size; L = left, R = right.

Regarding the FC between the rAI and regions within the DMN, we found that this seed was functionally connected with the traditional regions of the DMN in the three conditions, as can be observed in the table 7. Furthermore, the results showed that the FC between rAI and posterior regions of the DMN, namely PCC/precuneus was higher in the self and other conditions in comparison to the rest condition (see image 4). Additionally, connectivity between the rAI and the angular gyrus/TPJ was only observed in the self and other conditions.

Figure 4

Functional connectivity between right AI and DMN's regions in the three conditions

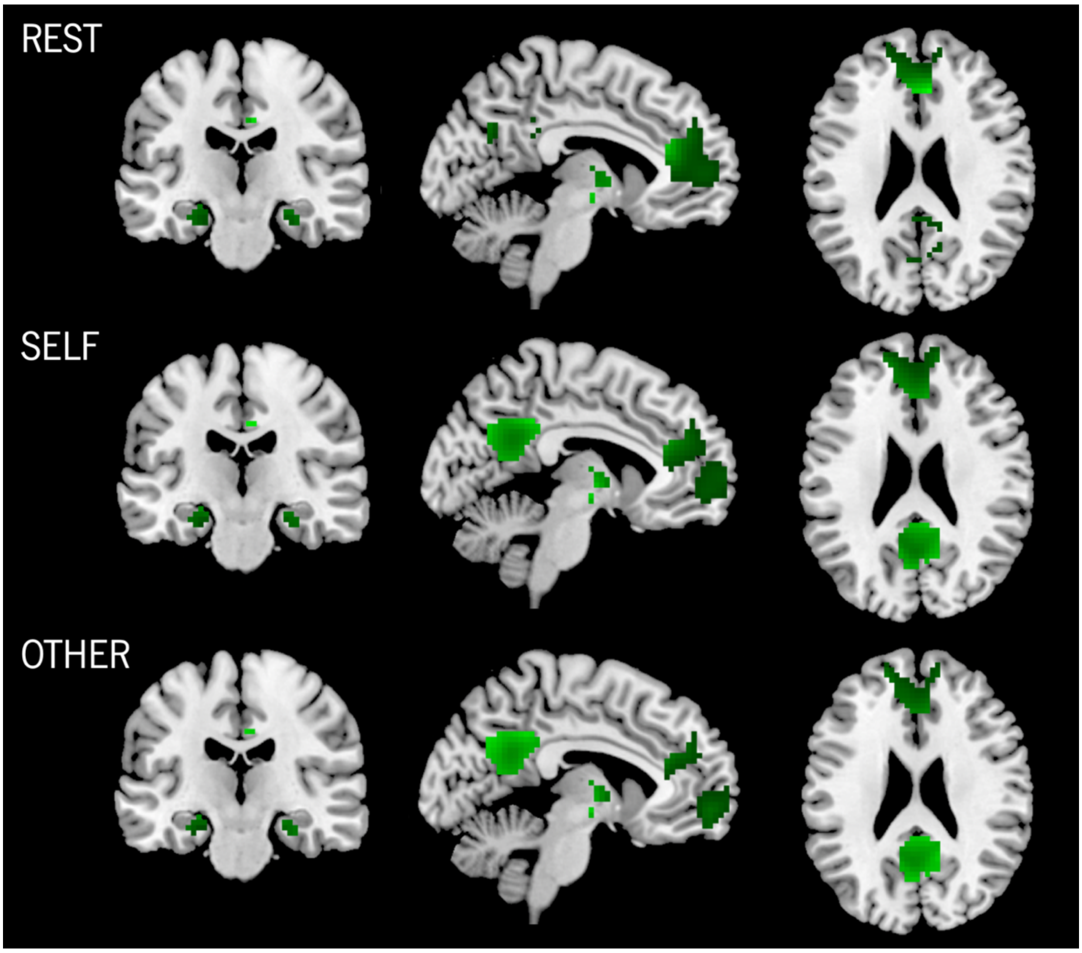

Note. p <.05 FWE corrected, extent threshold k=10 voxels.

Table 7

Functional connectivity between right AI and DMN's regions in the three conditions

		MNI Coordinates						**MNI Coordinates**						**MNI Coordinates**				
Seed	**Connected region**	**x**	**y**	**z**	**T**	**k**	**Connected region**	**x**	**y**	**z**	**T**	**k**	**Connected region**	**x**	**y**	**z**	**T**	**k**
R AI	*Resting*						*Self*						*Other*					
	R Anterior cingulate	6	30	21	26.38	626	R Middle cingulate	3	-21	39	28.29	34	L Lingual	-15	-30	-3	25.57	98
	L Middle frontal	-24	45	33	12.64		L Lingual	-15	-30	-3	26.12	103	L Parahippocampal	-21	-24	-12	12.72	
	L Superior frontal	-15	51	12	11.02		L Parahippocampal	-21	-24	-12	13.48		L Middle cingulate	0	-21	39	24.81	34
	R Middle cingulate	6	-18	36	22.22	34	L Precuneus	-3	-45	39	25.03	469	R Precuneus	12	-57	36	24.36	469
	L Thalamus	-6	-9	-6	20.28	67	R Posterior cingulate	3	-39	36	23.87		R Posterior cingulate	6	-60	15	23.63	
	R Thalamus	6	-9	-3	17.35		R Precuneus	9	-66	33	21.80		L Thalamus	-6	-9	-6	20.69	67
	L Lingual	-15	-30	-3	12.84	82	R Thalamus	6	-9	-3	24.84	67	R Thalamus	6	-15	3	20.34	
	L Parahippocampal	-21	-24	-12	9.33		L Thalamus	-6	-9	-6	20.56		L Superior frontal	-21	39	33	14.31	691
	R Precuneus	9	-66	33	11.01	111	L Superior frontal	-21	39	33	15.43	880	R Anterior cingulate	6	33	24	11.51	
	L Precuneus	-6	-66	33	9.23		R Anterior cingulate	6	33	24	14.69		R Angular/TPJ	48	-63	30	14.15	13
	R Parahippocampal	33	-30	-12	10.91	41	L Anterior cingulate	-3	33	24	13.99		L Angular/TPJ	-39	-66	33	13.03	25
							R Angular/TPJ	48	-63	30	14.92	13	R Parahippocampal	24	-30	-12	12.57	41
							R Parahippocampal	30	-33	-12	14.78	41	R Superior frontal	21	39	39	10.58	25
							R Superior frontal	21	39	39	13.52	29						
							L Angular/TPJ	-39	-66	33	12.64	19						

Note. p<.05 FWE corrected, extent threshold k=10 voxels; k=cluster size; L = left, R = right; TPJ = temporoparietal junction.

Association between DMN and SN's FC and self-report measures

We found that the total IRIC scores, as well as the cognitive subscale (PT) were positively correlated with the FC in the SMFG, whereas for the affective subscale (EC) the correlation was negative, with increased FC in the ventral ACC and right precuneus being associated with lower scores in the affective domain.

Regarding the SN, the significant correlations with IRIC were negative with increased FC in right middle frontal gyrus, right ACC, and SMFG being associated with decreased cognitive scores.

Detailed results can be seen in table 8.

Table 8

Correlations between DMN and SN functional connectivity and IRIC scores

				MNI coordinates					
	Scale	**Correlation**	**Region of interest**	**x**	**y**	**z**	**T**	***p***	**k**
DMN	*IRIC Total*	*Positive*	R Superior medial frontal	3	60	3	3.04	.002	146
			L Superior medial frontal	-3	54	21	2.64	.006	
	IRIC-PT	*Positive*	L Superior medial frontal	-12	48	6	3.69	.000	199
	IRIC-EC	*Negative*	L Ventral anterior cingulate	-6	39	0	4.28	.000	84
			R Ventral anterior cingulate	3	42	-3	3.39	.001	
			R Precuneus	3	-54	24	3.55	.001	87
SN	*IRIC Total*	*Negative*	R Middle frontal	24	39	24	3.37	.001	35
	IRIC-PT	*Negative*	R Middle frontal	27	39	30	3.66	.000	37
			R Anterior middle/ dorsal anterior cingulate	9	33	30	2.93	.003	84
			L Superior medial frontal	0	24	42	2.57	.007	
			L Superior frontal	-12	18	45	2.4	.011	

Note. p <.05 corrected for multiple comparisons, extent threshold of k=54 voxels for DMN and k=35 for SN; k = cluster size; L = left, R = right; IRIC = Interpersonal Reactivity Index for Couples; PT = perspective taking; EC = empathic concern.

Image 5

Correlations between DMN and SN functional connectivity and IRIC scores

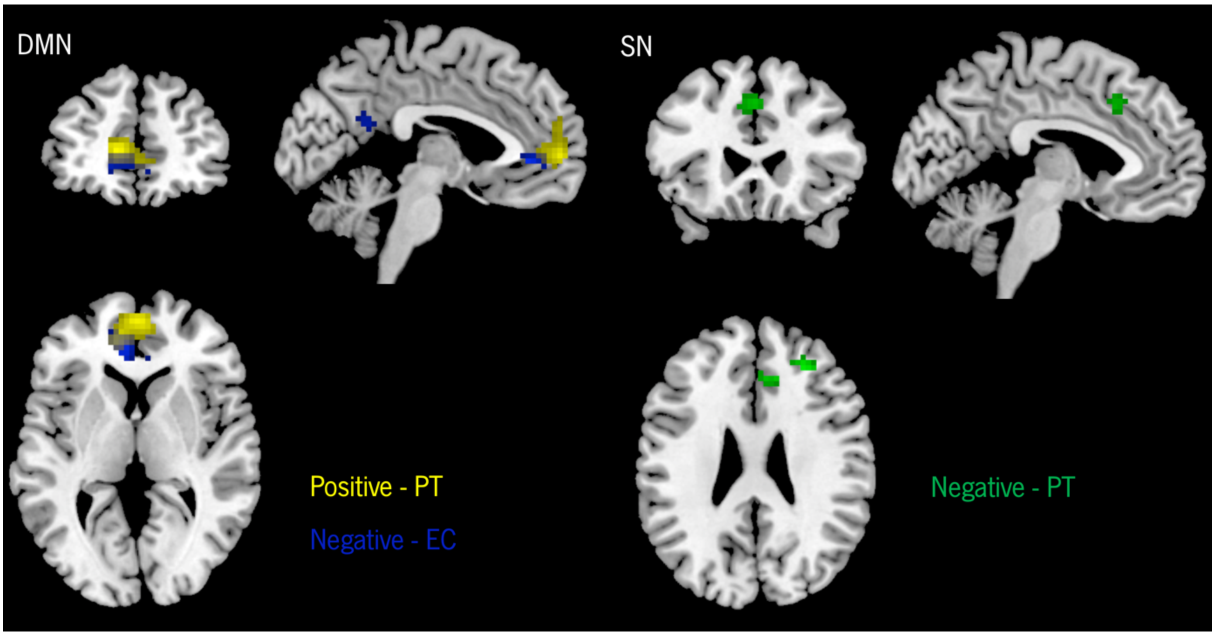

Note. *p* <.05 corrected for multiple comparisons, extent threshold of k=54 voxels for DMN and k=35 for SN; PT = perspective taking; EC = empathic concern.

Discussion

In the present study, we aimed at analyzing the FC of the DMN and SN, both during resting state and performance of a socio-cognitive task towards a romantic close other. This task included a self condition, in which participants had to elaborate on their own experience, and an other condition in which they elaborated on the experience of their partner. Thus, we compared the FC patterns of these two SC related networks in the three conditions – rest condition, self condition, and other condition - using two complementary methods of FC analysis: ICA and seed-based correlational analyses. Additionally, we looked at the interplay between the two networks across conditions to better understand how the dynamic interaction across the socio-cognitive (DMN) and socio-affective (SN) brain systems changes from rest to social task performance.

In terms of the connectivity pattern of the DMN, accessed via ICA, we found that the network's main nodes were functionally connected in the three conditions. As expected, and considering the key role of the DMN as a mentalizing system, we found that the network's pattern changed in the transition from resting state to self and other processing, with the overall FC being higher during task performance in comparison to rest. These results are consistent with a metanalysis by Alcalá-López and colleagues

(2018) in which an increase in the strength of DMN´s intra-network connectivity in task performance compared to resting state had also been reported. In the same line, a recent work by Wang and colleagues (2021) on the structural and functional connectome of the social mentalizing network reported an increase in the FC of areas such as the dorsal MPFC, ventral MPFC, TPJ, and precuneus with the augmented demands of the mentalizing task. Thus, these results confirm the well-known relationship between the DMN, as the mentalizing system in SC, and our ability to infer internal states, either ours or the ones of others (Knyazev et al., 2020).

Moreover, during both rest and self conditions, we observed relatively higher connectivity in anterior regions of the DMN, namely in ventral ACC and left SMFG, whereas in the other condition the higher connectivity was observed in posterior regions, namely in PCC/precuneus. This finding is consistent with the evidence for an anterior-posterior dissociation of the DMN, found in previous research (Coutinho et al., 2015b), pointing to a functional specialization within the network, with the anterior portions more involved in self-referential processes and the posterior areas involved in episodic memory and perceptual processing. Similarly, Murray and colleagues (2015) refer to the pregenual ACC as the seed node for a conceptual self network and the PCC/precuneus as the seed for a conceptual other network.

In respect to the SN, the network also presented its typical FC pattern across the three conditions. The observed main difference, however, suggested a more limited FC in key nodes, such as the dACC and AI in the other condition compared to rest and self. This suggests that when left to think freely or explicitly told to think about their internal states, subjects tended to recruit to a greater extent the emotional circuits subserved by the SN. Furthermore, this finding aligns with our hypothesis and the well-known association between the SN and self-referential interoceptive processes (Timmers et al., 2018). Similar evidence was reported by Cheng et al. (2010), in which subjects watched painful situations and had to imagine them from a self, loved-one, and stranger perspective. Although the three perspectives were related to a neural network of pain processing, activation in the AI and ACC showed a gradient decline from the self, to close other, and to the stranger (Cheng et al. 2010).

Having characterized the functional architecture of each network, we proceeded to the analysis of the interplay between them. Using a seed-based approach to see how the DMN interacts with the SN, we intended to better understand the integration between cognitive and emotional dimensions of SC both during rest and during the task performance.

As hypothesized, our results pointed to an interplay between the two networks in the three conditions. Importantly, both self and other conditions showed a higher FC between the MPFC (the selected DMN seed region) and the nodes of the SN - AI and dACC - pointing to increased functional interaction between both networks when the subjects were actively involved in a social task. This suggests greater integration between affective, or bottom-up, and cognitive, or top-down, dimensions during the socio-processing. Likewise, in a review on the types of brain network organization that occurs in the context of SC, Schurz et al. (2021) concluded that increased network integration indicated more effortful and controlled processing. Shine and collaborators (2016) also reported that network integration increased in a theory of mind task compared to passive rest, leading the authors to conclude that in response to task complexity, large-scale brain networks increase their integration as a response to task complexity (Shine & Poldrack, 2018).

Interestingly, we only observed FC between the MPFC and cerebellum during task performance, which is in line with the documented role of the cerebellum for SC, supported by results of cerebellar activation during empathy and mentalizing tasks (Jackson et al., 2005; Moriguchi et al., 2007) and by evidence from lesions studies showing that cerebellar damage results in deficits in theory of mind (Clausi et al., 2019; Gerschcovich et al., 2011).

When using the right AI as the seed region, we replicated the coupling between the SN and the DMN across conditions. This is not surprising due to the role of the AI in coordinating the switching between large scale networks, namely the DMN and the central executive network (Menon & Uddin, 2010). Moreover, we observed that the increased connectivity between the SN and the DMN was more evident with posterior nodes of the DMN, namely the lingual/parahippocampal/hippocampus, PCC/precuneus, and MCC. The connection with hippocampal regions during task performance may reflect the retrieval of memories of past experiences (Aminoff et al., 2013; Laurita et al. 2017), needed for this task in which subjects may have evoked specific episodic memories related to the content depicted in the videos.

Notably, it was only in the task-dependent conditions that the rAI increased its connectivity with regions such as the angular gyrus/TPJ, which correspond to DMN's areas involved in the cognitive representation of both self and other´s internal states and self-other distinction (Eddy, 2016; Santiesteban et al., 2012). As suggested by Qin et al. (2020), connectivity between the insula and TPJ could serve the association between internal and external aspects of the self, which could serve as the basis for further co-representation of social information pertaining to both self and other.

In a study where subjects observed strangers and close others experiencing painful stimulus, Cheng et al. (2010) found that the closer the relationship between the observer and the target, the greater the right TPJ deactivation and the higher the activation in the AI. According to the authors, this TPJ deactivation may reflect the increased self-other blending that characterizes empathic processes towards close others. The same process of inclusion the other in the self may have influenced our results in which the target was an intimate other. This leads us to infer that if we had included another experimental condition in which the target was a distant or non-familiar other, we would find a higher FC with the TPJ and this difference would be more pronounced for the distant other compared to the self or close other condition.

Finally, the greater involvement of the DMN in the cognitive route and of the SN in the affective route of SC was confirmed by the results from the correlational analysis between their FC pattern at rest and self-perceived empathic abilities. While the DMN was positively associated with IRIC cognitive scores and negatively associated with affective scores, the SN was negatively associated with cognitive IRIC scores. This adds to previous work of our research team (Oliveira-Silva et al., 2018), in which the superior MPFC, was positively associated with higher scores in the cognitive domain, and negatively associated with higher scores in the affective domain.

In summary, this study provided some insight into the configuration of two key social networks across different brain states. Taken together our findings showed that intra and inter-network connectivity increased from resting to task, supporting the need for a higher integration between different social brain areas during the active processing of social information. On the other hand, the focus on the other´s experience seems to have increased the recruitment of posterior areas, with the connectivity within the DMN being higher in posterior nodes such as the PCC/precuneus, and the connectivity within key SN nodes such as the AI being also relatively lower in the other condition. Finally, the AI was more connected with DMN posterior nodes and the recruitment of the cerebellum was more evident in the other.

Limitations and future directions

The present work used FC methods to describe the relationship between nodes of the DMN and SN. FC methods are based on the correlations between brain regions' BOLD signal fluctuations over time, and despite its utility and extensive use in the literature, they can be complemented by other approaches. One of those complementary methods is dynamic functional connectivity, which contrarily to FC that is based on the assumption of stationarity, addresses the temporal component (fluctuations) of spontaneous BOLD signals (Cabral et al., 2011; Soares et al., 2016)

On the other hand, despite its utility and ability to detect consistent spatiotemporal relationships between different brain regions, they don´t assess the directed influence that one brain area exerts over another. Thus, this can be accomplished through effective connectivity analyses (Friston, 1994) which, as showed in previous work (Esménio et al., 2020), considers how the information flows through brain regions of a given network as well as between networks (Friston, 2011). For instance, the knowledge of the information flow between socio-affective and socio-cognitive networks will clarify if they are hierarchically related, with the ability to abstract mental state attributions being dependent on the ability to simulate the other state.

The relative homogeneity of our sample in terms of age, relationship duration, and marital functioning may also be seen as a possible limitation of the present work, which restricts the generalization of our findings to similar samples of relatively young and healthy couples. This may be important considering that variables such as relationship duration and associated level of interpersonal closeness (Cheng et al., 2010) may modulate the overlap between self and other neural representations. Thus, future studies should measure or experimentally manipulate relationship factors that may modulate the socio-cognitive and socio-affective routes towards close others.

Finally, and although this study may have implications for couples' research, it would be interesting to examine the existence of similar connectivity patterns in other dyads, such as parent-child or therapist-patient exchanges.

References

Alcalá-López, D., Smallwood, J., Jefferies, E., Van Overwalle, F., Vogeley, K., Mars, R. B., Turetsky, B. I., Laird, A. R., Fox, T. P., Eickhoff, S. B., & Bzdok, D. (2018). Computing the social brain connectome across systems and states. *Cerebral Cortex, 28*(7), 2207-2232. https://doi.org/10.1093/cercor/bhx121

Alcalá-López, D., Vogeley, K., Binkofski, F., & Bzdok, D. (2019). Building blocks of social cognition: Mirror, mentalize, share?. *Cortex, 118*, 4-18. https://doi.org/10.1016/j.cortex.2018.05.006

Amft, M., Bzdok, D., Laird, A. R., Fox, P. T., Schilbach, L., & Eickhoff, S. R. (2015). Definition and characterization of an extended social-affective default network. *Brain Structure and Function, 220*, 1031-1049. http://doi.org/10.1007/s00429-013-0698-0

Aminoff, E.M., Kveraga, K., Bar, M. (2013). The role of the parahippocampal cortex in cognition. *Trends in Cognitive Sciences, 17*(8), 379–90. https://doi.org/10.1016/j.tics.2013.06.009

Ashburner, J. (2007). A fast diffeomorphic image registration algorithm. *Neuroimage, 38*(1), 95-113. https://doi.org/10.1016/j.neuroimage.2007.07.007

Beckmann, C., DeLuca, M., Devlin, J. T., & Smith, S. M. (2005). Investigations into resting-state connectivity using independent component analysis. *Philosophical Transactions of the Royal Society B, 360*(1457), 1001-1013. http://doi.org/10.1098/rstb.2005.1634

Bell, A. J., & Sejnowski, J. T. (1995). An information-maximization approach to blind separation and blind deconvolution. *Neural Computation, 7*(6), 1129–1159. https://doi.org/10.1162/neco.1995.7.6.1129

Buckner, R. L. (2012). The serendipitous discovery of the brain's default network. *Neuroimage, 62*(2), 1137-1145. https://doi.org/10.1016/j.neuroimage.2011.10.035

Bzdok, D., Schilbach, L., Vogeley, K., Scheider, K., Laird, A. R., Langner, R., & Eickhoff, S. R. (2012). Parsing the neural correlates of moral cognition: ALE meta-analysis on morality, theory of mind, and empathy. *Brain Structure and Function, 217*, 783-796. https://doi.org/10.1007/s00429-012-0380-y

Cabral, J., Hugues, E., Sporns, O., and Deco, G. (2011). Role of local network oscillations in resting-state functional connectivity. *Neuroimage 57*(1), 130–139. https://doi.org/10.1016/j.neuroimage.2011.04.010

Calhoun, V.D., Adali, T., Pearlson G. D., & Pekar, J. J. (2001). Spatial and temporal independent component analysis of functional MRI data containing a pair of task-related waveforms. *Human Brain Mapping, 13*(1), 43–53. https://doi.org/10.1002/hbm.1024

Chao-Gan, Y., & Yu-Feng, Z. (2010). DPARSF: a MATLAB toolbox for "pipeline" data analysis of resting-state fMRI. *Frontiers in Systems Neuroscience, 4*, 13. https://doi.org/10.3389/fnsys.2010.00013

Cheng, Y., Chen, C., Lin, C. P., Chou, K. H., & Decety, J. (2010). Love hurts: an fMRI study. *Neuroimage 51*(2), 923–929. https://doi.org/10.1016/j.neuroimage.2010.02.047

Chiong, W., Wilson, S. M., D'Esposito, M., Kayser, A. S., Grossman, S. N., Poorzand, P., Seeley, W. W., Miller, B. L., & Rankin, K. P. (2013). The salience network causally influences default mode network activity during moral reasoning. *Brain a Journal of Neurology, 136*(6), 1929-1941. https://doi.org/10.1093/brain/awt066

Clausi, S., Olivito, G., Lupo, M., Siciliano, L., Bozzali, M., & Leggio, M. (2019). The cerebellar predictions for social interactions: theory of mind abilities in patients with degenerative cerebellar atrophy. *Frontiers in Cellular Neuroscience, 12*, 510. https://doi.org/10.3389/fncel.2018.00510

Cohen, S., Schulz, M. S., Weiss, E., & Waldinger, R. J. (2012). Eye of the beholder: The individual and dyadic contributions of empathic accuracy and perceived empathic effort to relationship satisfaction. *Journal of Family Psychology, 26*(2), 236–245. https://doi.org/10.1037/a0027488

Courtney, A. L., & Meyer, M. L. (2020). Self-other representation in the social brain reflects social connection. *The Journal of Neuroscience, 40*(29), 5616–5627. https://doi.org/10.1523/JNEUROSCI.2826-19.2020

Coutinho, J., Beiramar, A., Silva, C., Lema, A., Lima, V., Grace, R., Oliveira-Silva, P., Golçalves, O., & Sampaio, A. (2015a) Evidências de validade da versão portuguesa do índice de reatividade interpessoal para casais. Avaliação Psicológica, 14(3), 309–317. http://doi.org/10.15689/ap.2015.1403.02

Coutinho, J. F., Fernandesl, S. V., Soares, J. M., Maia, L., Gonçalves, Ó. F., & Sampaio, A. (2015b). Default mode network dissociation in depressive and anxiety states. *Brain Imaging and Behavior, 10*(1), 147–157. https://doi.org/10.1007/s11682-015-9375-7

Coutinho, J., Oliveira-Silva, P., Fernandes, E., Gonçalves, O. F., Correia, D., Perrone Mc-Govern, K., & Tschacher, W. (2018). Psychophysiological synchrony during verbal interaction in romantic relationships. *Family Process, 58*(3), 716-733. https://doi.org/10.1111/famp.12371

Coutinho, J., Oliveira-Silva, P., Mesquita, A. R., Barbosa, M., Perrone-Mcgovern, K. M., & Gonçalves, O. F. (2017). Psychophysiological reactivity in couples during a marital interaction task. *Applied Psychophysiology and Biofeedback, 42*, 335–346. https://doi.org/10.1007/s10484-017-9380-2

Coutinho, J. F., Sampaio, A., Ferreira, M., Soares, J. M., & Gonçalves, O. F. (2013). Brain correlates of pro-social personality traits: a voxel-based morphometry study. *Brain Imaging and Behavior, 7*, 293-299. https://doi.org/10.1007/s11682-013-9227-2

Craig, A. D. B. (2010). The sentient self. *Brain Structure and Function, 214*, 563–577. https://doi.org/10.1007/s00429-010-0248-y

Davis, M. H. (1980). A multidimensional approach to individual differences in empathy. *JSAS Catalog of Selected Documents in Psychology, 10*, 85. https://www.uv.es/friasnav/Davis_1980.pdf

de Vignemont, F., & Singer, T. (2006). The empathic brain: how, when and why?. *Trends in Cognitive Sciences, 10*(10), 435–441. https://doi.org/10.1016/j.tics.2006.08.008

Di, X., & Biswal, B. B. (2014). Identifying the default mode network structure using dynamic causal modeling on resting-state functional magnetic resonance imaging. *Neuroimage, 86*, 53-59. http://dx.doi.org/10.1016/j.neuroimage.2013.07.071

Eddy, C.M. (2016). The junction between self and other? temporo-parietal dysfunction in neuropsychiatry. *Neuropsychologia 89*, 465–477. https://doi.org/10.1016/j.neuropsychologia.2016.07.030

Esménio, S., Soares, J. M., Oliveira-Silva, P., Gonçalves, Ó. F., Decety, J., & Coutinho, J. (2019a). Brain circuits involved in understanding our own and other's internal states in the context of romantic relationships. *Social Neuroscience, 14*(6) 729–738. https://doi.org/10.1080/17470919.2019.1586758

Esménio, S., Soares, J. M., Oliveira-Silva, P., Gonçalves, Ó. F., Friston, K., & Coutinho, J. (2020). Changes in the effective connectivity of the social brainwhen making inferences about close others vs. the self. *Frontiers in Human Neuroscience, 14*, 151. https://doi.org/10.3389/fnhum.2020.00151

Esménio, S., Soares, J. M., Oliveira-Silva, P., Zeidman, P., Razi, A., Goncalves, O. F., Friston, K., & Coutinho, J. (2019b). Using resting-state DMN effective connectivity to characterize the neurofunctional architecture of empathy. *Scientific Reports, 9*(2603), https://doi.org/10.1038/s41598-019-38801-6

Fallon, N., Roberts, C., & Stancak, A. (2020). Shared and distinct functional networks for empathy and pain processing: a systematic review and meta-analysis of fMRI studies. *Social Cognitive and Affective Neuroscience, 15*(7), 709–723. https://doi.org/10.1093/scan/nsaa090

Fan, Y., Duncan, N. W., de Greck, M., & Northoff, G. (2011). Is there a core neural network in empathy? An fMRI based quantitative meta-analysis. *Neuroscience and Biobehavioral Reviews, 35*(3), 903-911. https://doi.org/10.1016/j.neubiorev.2010.10.009

Friston, K. J. (1994). Functional and effective connectivity in neuroimaging: a synthesis. *Human. Brain Mapping, 2*(1-2), 56–78. https://doi.org/10.1002/hbm.460020107

Friston, K. J. (2011). Functional and effective connectivity: a review. *Brain Connectivity, 1*(1), 13–36. https://doi.org/10.1089/brain.2011.0008

Frith, C., & Frith, U. (2005). Theory of mind. *Current Biology, 15*(17), R644–R645. https://www.cell.com/current-biology/pdf/S0960-9822(05)00960-7.pdf

Gerschcovich, E. R., Cerquetti, D., Tenca, E. & Leiguarda, R. (2011). The impact of bilateral cerebellar damage on theory of mind, empathy and decision making. *Neurocase 17*(3), 270–275. https://doi.org/10.1080/13554791003730618

Greicius, M. D., Krasnow, B., Reiss, A. L., Menon, V. (2003). Functional connectivity in the resting brain: a network analysis of the default mode hypothesis. *Proceedings of the National Academy of Sciences of the United States of America, 100*(1), 253-258. https://doi.org/10.1073/pnas.0135058100

Huang, Z., Obara, N., DavisIV, H. H., Pokorny, J., & Northoff, G. (2016). The temporal structure of resting-state brain activity in the medial prefrontal cortex predicts self-consciousness. *Neuropsychologia, 82*, 161-170. http://dx.doi.org/10.1016/j.neuropsychologia.2016.01.025

Laurita, A. C., Hazan, C., & Spreng, R. N. (2017). Dissociable patterns of brain activity for mentalizing about known others: a role for attachment. *Social Cognitive and Affective Neuroscience*, *12*(7),1072–1082, https://doi.org/10.1093/scan/nsx040

Li, W., Mai, X., & Liu, C. (2014). The default mode network and social understanding of others: what do brain connectivity studies tell us. *Frontiers in Human Neuroscience, 8*, 74. https://doi.org/10.3389/fnhum.2014.00074

Lieberman, M. D., Straccia, M. A., Meyer, M.L., Du, M., & Tan, K. M. (2019). Social, self, (situational), and affective processes in medial prefrontal cortex (mPFC): causal, multivariate, and reverse inference evidence. *Neuroscience and Biobehavioral Reviews, 99*, 311–328. https://doi.org/10.1016/j.neubiorev.2018.12.021

López-Solà, M., Koban, L., Krishnan, A., & Tor Wager, T. D., (2020). When pain really matters: A vicarious-pain brain marker tracks empathy for pain in the romantic *partner. Neuropsychologia 145*, 106427. https://doi.org/10.1016/j.neuropsychologia.2017.07.012

Jackson, P. L., Meltzoff, A. N. & Decety, J. (2005). How do we perceive the pain of others? a window into the neural processes involved in empathy. *Neuroimage, 24*(3), 771–779. https://doi.org/10.1016/j.neuroimage.2004.09.006

Kanske, P., Böckler, A., Trautwein, F.-M., Parianen Lesemann, F. H., & Singer, T. (2016). Are strong empathizers better mentalizers? Evidence for independence and interaction between the routes of social cognition. *Social Cognitive and Affective Neuroscience, 11*(9), 1383-1392. https://doi.org/10.1093/scan/nsw052

Kanske, P., Böckler, A., Trautwein, F.-M., & Singer, T. (2015). Dissecting the social brain: Introducing the EmpaToM to reveal distinct neural networks and brain-behavior relations for empathy and theory of mind. *NeuroImage, 122*, 6–19. http://dx.doi.org/10.1016/j.neuroimage.2015.07.082

Knyazev, G. G., Savostyanov, A. N., Bocharov, A. V., Levin, E. A., & Rudych P. D. (2020). Intrinsic connectivity networks in the self- and other-referential processing. *Frontiers in Human Neuroscience, 14*, 460. https://doi.org/10.3389/fnhum.2020.579703

Krienen F. M., Tu P. -C., & Buckner R. L. (2010). Clan mentality: evidence that the medial prefrontal cortex responds to close others. *Journal of Neuroscience, 30*(41), 13906–13915. https://doi.org/10.1523/JNEUROSCI.2180-10.2010

Mars, R. B., Neubert, F. X., Noonan, M. P., Sallet, J., Toni, I., & Rushworth, M. F. (2012). On the relationship between the "default mode network" and the "social brain". *Frontiers in Human Neuroscience, 6*, 189. https://doi.org/10.3389/fnhum.2012.00189

Meyer, M. L. (2019). Social by default: characterizing the social functions of the resting brain. *Current Directions in Psychological Science, 28*(4), 380-386. https://doi.org/10.1177/0963721419857759

Meyer, M. L., & Lieberman, M. D. (2018). Why people are always thinking about themselves: medial prefrontal cortex activity during rest primes self-referential processing. *Journal of Cognitive Neuroscience, 30*(5), 714–721. https://doi.org/10.1162/jocn_a_01232

Meyer, M. L., Masten, C. L., Ma, Y., Wang, C., Shi, Z., Eisenberger, N. I., & Han, S. (2013). Empathy for the social suffering of friends and strangers recruits distinct patterns of brain activation. Social Cognitive and Affective Neuroscience, 8(4), 446-454. https://doi.org/10.1093/scan/nss019

Menon, V. (2015). Salience network. *Brain Mapping: An Encyclopedic Reference, 2*, 597-611. https://doi.org/10.1016/B978-0-12-397025-1.00052-X

Menon, V., & Uddin, L. Q. (2010). Saliency, switching, attention and control: A network model of insula function. *Brain Structure & Function, 214*(5-6), 655-667. https://doi.org/10.1007/s004290100262-0

Moriguchi, Y., Decety, J., Ohnishi, T., Maeda, M., Mori, T., Nemoto, K., Matsuda, H., & Komaki, G. (2007). Empathy and judging other's pain: nn fMRI study of alexithymia. *Cerebral Cortex, 17*(9), 2223–2234. https://doi.org/10.1093/cercor/bhl130

Murray, R.J., Debbané, M., Fox, P.T., Bzdok, D., & Eickhoff, S.B. (2015). Functional connectivity mapping of regions associated with self- and other-processing. *Human Brain Mapping, 36*(4), 1304-1324. https://doi.org/10.1002/hbm.22703

Nomi, J. S., Farrant, K., Damaraju, E., Rachakonda, S., Calhoun, V.D. & Uddin, L.Q. (2016), Dynamic functional network connectivity reveals unique and overlapping profiles of insula subdivisions. *Human Brain Mapping, 37*, 1770-1787. https://doi.org/10.1002/hbm.23135

Northoff, G., Duncan, N. W., & Hayes, D. J. (2010). The brain and its resting state activity — experimental and methodological implications. *Progress in Neurobiology, 92*(4), 593-600. https://doi.org/10.1016/j.pneurobio.2010.09.002

Oliveira-Silva, P., Maia, L., Coutinho, J., Frank, B., Soares, J. M., Sampaio, A., & Gonçalves, Ó. F. (2018). Empathy by default: Correlates in the brain at rest. *Psicothema, 30*(1), 97-103. http://doi.org/10.7334/psicothema2016.366

Péloquin, K. & Lafontaine, M. F. (2010). Measuring empathy in couples: Validity and reliability of the interpersonal reactivity index for couples. *Journal of Personality Assessment, 92*(2), 146–157. https://doi.org/10.1080/00223890903510399

Qin, P., Wang, M., & Northoff, G. (2020). Linking bodily, environmental and mental states in the self—a three-level model based on a meta-analysis. *Neuroscience and Biobehavioral Reviews 115*, 77-95. https://doi.org/10.1016/j.neubiorev.2020.05.004

Raichle, M. E. (2015). The brain's default mode network. *Annual Review of Neuroscience, 38*, 433–447. https://doi.org/10.1146/annurev-neuro-071013-014030

Sampaio, A., Soares, J. M., Coutinho, J., Sousa, N., & Gonçalves, O. F. (2014). The big five default brain: functional evidence. *Brain Structure and Function, 219,* 1913-1922. https://doi.org/10.1007/s00429-013-0610-y

Santiesteban, I., Banissy, M. J., Catmur, C., & Bird, G. (2012). Enhancing social ability by stimulating right temporoparietal junction. *Current Biology, 22*(23), 2274–2277. http://dx.doi.org/10.1016/j.cub.2012.10.018

Schilbach, L., Bzdok, D., Timmermans, B., Fox, P. T., Laird, A. R., Vogeley, K., & Eickhoff, S. B. (2012). Introspective minds: using ALE meta-analyses to study commonalities in the neural correlates of emotional processing, social & unconstrained cognition. *Plos One, 7*(2), Article e30920. https://doi.org/10.1371/journal.pone.0030920

Schilbach, L., Eickhoff, S. B., Rotarska-Jagiela, A., Fink, G. R., & Vogeley, K. (2008). Minds at rest? Social cognition as the default mode of cognizing and its putative relationship to the "default system" of the brain. *Consciousness and Cognition*, *17*(2), 457–467. https://doi.org/10.1016/j.concog.2008.03.013

Schurz, M., Maliske, L., & Kanske, P. (2021). Cross-network interactions in social cognition: a review of findings on task related brain activation and connectivity. Cortex, 130, 142-157. https://doi.org/10.1016/j.cortex.2020.05.006

Schurz, M., Radua, J., Aichhorn, M., Richlan, F., & Perner, J. (2014). Fractionating theory of mind: A meta-analysis of functional brain imaging studies. *Neuroscience and Biobehavioral Reviews, 42*, 9-34. https://doi.org/10.1016/j.neubiorev.2014.01.009

Schurz, M., Radua, J., Tholen, M. G., Maliske, L., Margulies, D. S., Mars, R. B., Sallet, J., & Kanske, P. (2020). Toward a hierarchical model of social cognition: a neuroimaging meta-analysis and integrative review of empathy and theory of mind. *Psychological Bulletin, 147*(3), 293-327. http://dx.doi.org/10.1037/bul0000303

Seeley, W. W., Menon, V., Schatzberg, A. F., Keller, J., Glover, G. H., Kenna, H., Reiss, A. L., & Greicius, M. D. (2007). Dissociable intrinsic connectivity networks for salience processing and executive control. *The Journal of Neuroscience, 27*(9), 2349 – 2356. https://doi.org/10.1523/JNEUROSCI.5587-06.2007

Shine, J. M., Bissett, P. G., Bell, P. T., Koyejo, O., Balsters, J. H., Gorgolewski, K. J., Moodie, C. A., & Poldrack, R. A. (2016). The dynamics of functional brain networks: Integrated network states during cognitive task performance. *Neuron, 92*(2), 544-554. https://doi.org/10.1016/j.neuron.2016.09.018

Shine, J. M., & Poldrack, R. A. (2018). Principles of dynamic network reconfiguration across diverse brain states. *NeuroImage, 180*, 396-405. https://doi.org/10.1016/j.neuroimage.2017.08.010

Soares, J. M., Magalhães, R., Moreira, P. S., Sousa, A., Ganz, E., Sampaio, A., Alves, V., Marques, P., & Sousa, N. (2016). A hitchhiker's guide to functional magnetic resonance imaging. Frontiers in *Neuroscience, 10*(515). https://doi.org/10.3389/fnins.2016.00515

Spunt, R. P., Meyer, M.L., & Lieberman, M. D. (2015). The default mode of human brain function primes the intentional stance. Journal of Cognitive Neuroscience, 27(6), 1116–1124. https://doi.org/10.1162/jocn_a_00785

Spreng, R. N., & Andrews-Hanna, J. R. (2015). The Default Network and Social Cognition. *Brain Mapping: An Encyclopedic Reference, 3*, 165-169. http://dx.doi.org/10.1016/B978-0-12-3970251.001731

Sevinc, G., Gurvit, R. & Spreng, R. N. (2017). Salience network engagement with the detection of morally laden information. *Social Cognitive and Affective Neuroscience*, 12(7), 1118-1127. https://doi.org/10.1093/scan/nsx035

Timmers, I., Park, A. L., Fischer, M. D., Kronman, C. A., Heathcote, L. C., Hernandez, J. M., & Simons, L. E. (2018). Is empathy for pain unique in its neural correlates? A meta- analysis of neuroimaging studies of empathy. *Frontiers in Behavioral Neuroscience, 12*, 289. https://doi.org/10.3389/fnbeh.2018.00289

Tzourio-Mazoyer, N., Landeau, B., Papathanassiou, D., Crivello, F., Etard, O., Delcroix, N., Mazoyer, B., & Joliot, M. (2002). Automated anatomical labeling of activations in SPM using a macroscopic anatomical parcellation of the MNI MRI single-subject brain. *NeuroImage, 15*(1), 273–289. https://doi.org/10.1006/nimg.2001.0978

Van Overwalle, F. (2009). Social cognition and the brain: A meta- analysis. *Human Brain Mapping, 30*(3), 829-858. https://doi.org/10.1002/hbm.20547

Von dem Hagen, E. A. H., Stoyanova, R. S., Baron-Cohen, S., & Calder, A. J. (2013). Reduced functional connectivity within and between "social" resting state networks in autism spectrum conditions. Social Cognitive and Affective *Neuroscience, 8*(6), 694-701. http://doi.org/10.1093/scan/nss053

Waldinger, R. J., Hauser, S. T., Schulz, M. S., Allen, J. P., & Crowell, J. A. (2004). Reading others emotions: The role of intuitive judgments in predicting marital satisfaction, quality, and stability. *Journal of Family Psychology, 18*(1), 58–71. https://doi.org/10.1037/0893-3200.18.1.58

Walter, H. (2012). Social cognitive neuroscience of empathy: concepts, circuits, and genes. Emotion Review, 4(1), 9-17. https://doi.org/10.1177/1754073911421379

Wang, Y., Metoki, A., Xia, Y., Zang, Y., He, Y., & Olson, I. R. (2021). A large-scale structural and functional connectome of social mentalizing. *NeuroImage, 236*, 118115. https://doi.org/10.1016/j.neuroimage.2021.118115